RESEARCH PAPER

Gold Nanoparticle Parameters Play an Essential Role as CT Imaging Contrast Agents

Mohsen Asadinezhad [1], Hosein Azimian [2], Hossein Ghadiri [3], Sara Khademi [1]*

[1] *Department of Radiology Technology, School of Paramedical Sciences, Mashhad University of Medical Sciences, Mashhad, Iran*

[2] *Medical Physics Research Center, Mashhad University of Medical Sciences, Mashhad, Iran*

[3] *Department of Medical Physics and Biomedical Engineering, Tehran University of Medical Sciences, Tehran, Iran*

ARTICLE INFO

ABSTRACT

Computed tomography (CT) is extensively used in clinical imaging modalities. There have recently been many reports to motivate for developing newer contrast agents. As a new contrast agent, gold nanoparticles (GNPs) have gained recent attention. In this paper, the effects of parameters related to gold nanoparticles (sizes, shapes, concentrations, and surface chemistries) on X-ray attenuation beam in human nasopharyngeal cancer cells were investigated. Hematoxylin and eosin (H&E), Colony, and MTT assays were applied to measure the compatibility of the NPs in cells. Our findings indicated that the GNPs with Au core sizes of ~13 nm and ~60 nm and polyethylene glycol covering on gold nanorods (PEG-GNRs) are non-cytotoxic and GNRs with an aspect ratio of 2.4 and 4.2 are toxic in a concentration range. At 80 kVp, GNPs (13 nm) enables 3.03–times higher contrast than iodine at a concentration of 5000 μM. The GNPs (13 nm) X-ray attenuations were 2.55-times and 1.63-times higher than PEG-GNRs and GNPs (60 nm) in cancer cells, respectively. X-ray attenuation highly increased when the concentration of mass (measured by ICP-OES) of NPs was elevated. In sum, smaller spherical GNPs can be proposed as an excellent possibility to Omnipaque for CT imaging of nasopharyngeal cancer cells.

How to cite this article

INTRODUCTION

CT is one of the commonly beneficial diagnostic modalities in clinics[1]. Currently, due to its high availability, accuracy, efficiency, 3D imaging ability**,** and cost. Usually, elements with a high density and atomic number tend to attenuate X-rays more incredible. Soft tissues are generally composed of carbon, oxygen and hydrogen, not good ability to attenuate X-ray. Therefore, contrast media containing elements with high electron density , and atomic number are essential for imaging with the more excellent contrast in CT[2]. The most generally used CT contrast media are small molecular iodine-based compounds, including Omnipaque. However, those iodine-based compounds have short blood circulation and imaging time , and when injected at high concentration, side effects including, anaphylactic shock, itching and vomiting limit their extensive use , and have also recently been linked to amplification in DNA damage[3]. Therefore, gold nanoparticles (GNPs) have gained attention as CT

* Corresponding Author Email: khademisr@mums.ac.ir

contrast agents because of their biocompatibility and high X-ray attenuation coefficient[4]. As was first demonstrated, gold induces a strong X-ray attenuation (XA), by Wilhelm Roentgen, in the first X-ray human image (Hand with Ring). In addition, GNPs have unique chemical, physical and biological virtues, which make them an excellent candidate for CT imaging contrast agents[5]. Because the atomic number (A) and electron density (ED) of gold (79 and 19.32 g/cm3, respectively) are more signiant than iodine molecules (53 and 4.9 g/cm3); therefore, various materials in the body prepare different levels of XA[6]. Ease of the surface functionalization; make GNPs as potentially promising multifunctional contrast media for medical imaging. In a series of biomedicine applications of GNPs, its duty in tumor diagnosis is individually outstanding.[5] In order to make GNPs more appropriate for tumor diagnosis, their properties should be understood. For better diagnostic CT imaging of the body, suitable GNPs are required to improve medical imaging precision, which has achieved a serious question for researchers and physicians. It is beneficial and essential to assess whether different specifications of GNPs could be applied to ameliorate contrast and absorbtion enhancement in cells. In addition, GNPs provide a high grade of flexibility in the phrase of functional groups for targeting and coating, and proved to be biocompatible. Based on Moghimi and et al. the way of materials in the body can be impacted by density**,** size, surface characteristics, and morphology of nanoparticles[7]. GNPs with polyethylene glycol (PEG) as a Surface functionalization have been widely performed. PEGylated GNPs (PEG-GNPs) reveal longer blood circulation time in vivo than bare GNPs[8]. Since the PEG chain length can influence blood circulation time; for example, GNPs with Au core size of 18 nm covered with 2 kDa PEG molecules show a circulation time of 4 h, while with 10 kDa PEG molecules they revealed a circulation time of nearly 51h[8, 9]. The present study aimed to investigate the effect of concentration, surface chemistry, size, and morphology of GNPs on XA beam in human nasopharyngeal cancer cells. To this end, firstly, the cytotoxic effect of the NPs was evaluated on two different cell lines (cancer and normal cells) in various concentrations. Afterward, the XA of NPs evaluated on nasopharyngeal cancer cells and compared with Omnipaque. Finally, the concentration of NPs in cells was confirmed by ICP-OES analysis.

MATERIALS AND METHODS
Materials
The GNPs, GNRs , and PEG-GNRs nanoparticles were prepared and synthesized as reported previously[10]. The water with a resistivity of 18.2MΩ cm was purified using a Milli-Q Plus machine (Millipore, MA). KB (nasopharyngeal cancer) and normal human dermal fibroblasts (HDFs) cells were purchased from the Institute of Pasteur in Iran. Fetal Bovine Serum (FBS) was prepared from BioSera Ltd (United Kingdom), and cells were cultured in RPMI (GIBCO (Invitrogen, Germany)) with 10% FBS. Dimethyl sulfoxide (DMSO), MTT, and gold salt ($HAuCl_4$) were prepared from Sigma Aldrich.

Characterization of NPs techniques
In the previous study, Transmission Electron Microscopy (TEM) was carried out applying a Zeiss EM 900 to evaluate the size and shape of NPs[10]. The UV-visible spectra were measured by spectrophotometer (SPEKOL 2000, UK) [10]. Inductively Coupled Plasma Optical Emission Spectrometry (ICP-OES) was applied to investigate the concentrations of NPs in μg/ml. Raman Spectrometer (Netherlands) was also used to determine the chemical composition of materials.

Toxicity test of the NPs
MTT assay
MTT assay measured the metabolic viability of the treated cells with GNPs (13 nm), GNPs (60 nm), PEG-GNR, GNRs with an aspect ratio (AR) 2.4, GNRs with AR 4.2 at different concentrations range (0, 200, 300, 400, 500 μM). 1×10^4 KB cells were seeded per well for 24 h. After 24 h, the RPMI medium in the plates was removed and fresh medium containing NPs at various concentrations added, then cultured at 37 °C for 24 h. After that, the solution of MTT (Sigma-Aldrich, USA) at sufficient concentrations were added to each well. Following incubation for 4 h, the solution was replaced with nearly 200 μl of DMSO. The absorbances were measured at 570 nm. After 24 h, Cell toxicity was determined and compared to the control cells (100% viability: the absorbance of the control cells).

Colony assay
For long-term cytotoxicity (colony formation

assay (CFA)), the density of $5×10^3$ KB cells/well were cultured with and without GNPs (13 nm) at the concentration of 500μM for 24h incubation. After washing cells with PBS and added RPMI with 10% FBS, the plates were maintained in a humid incubator. After10 days, Giemsa staining was done to show the colonies. The number of colonies was counted. Percentage of plate efficiency (PE) and percentage of surviving fraction (SF) were calculated using the following formula:

$$\%PE = \frac{Number\ of\ colonies\ formed}{Number\ of\ cells\ seeded} ×100 \quad 1 \quad (1)$$

$$\%SF = \frac{Number\ of\ colonies\ after\ treatment}{Number\ of\ cells\ seeded ×PE} ×100 \quad (2)$$

H&E

The cytotoxicity of the GNPs (13 nm) was further examined by cell morphology observation after H&E staining. In Brief, $2×105$ HDF cells were seeded into each well of 6-well plates. After 24 h, the medium was replaced with a fresh medium containing GNPs (13 nm) with concentrations of 0, and 500 μM, and the cells were incubated for 24 h at 37 °C. After washing with PBS, the cells were fixed in 4% paraformaldehyde for 2 h. Then, the cells were washed with PBS. Then, hematoxylin was added; after 30 s, the cells were washed with PBS and stained with 1% eosin solution for 10–30 s. Finally, the cells were dehydrated. The cell morphology was observed using an optical microscope.

CT scanning of nasopharyngeal cancer cells

One×10^6 KB cells/ well were cultured in 6-well plates (in triplicate.) Then, KB cells were seeded with GNPs (13 nm), GNPs (60 nm), and PEG-GNR at concentrations of (0-500) μM, respectively and incubated at 37 °C and 5% CO_2 for 24h. After three times washing KB cells with PBS, then, the KB cells were separated with trypsin, removed trypsin with a centrifuge, and suspended in Eppendorf tubes with nearly 100 μl PBS. Afterward, the KB cells resuspension in each of the Eppendorf tubes was located in an imaging holding device that was self-designed (made of poly-methyl-methacrylate (PMMA)) and scanned by a 64-slice hospital imaging modality (VCT, GE Healthcare). The operating parameters are the following:

1. X-ray tube potentials: 80 kVp, 2. exposure time: 1000 ms, 3. slice thickness: 0.625 mm, 4. display field of view: 130×130 mm, 5. Scan field of view: 250×250 mm, 6. pitch: 1 and 7. Tube current: 300 mA. The CT value or X-ray absorbtion pixel value in Hounsfield Units (HU) of NPs was determined for the uniform circular region of interest (ROI) located on the image of CT.

Cellular uptake assessments

Nanoparticle cell uptake was investigated using ICP-OES. The KB cells at a density of $1×10^6$ cells/well were cultured in 6-well plates. After 24 h, the (GNPs (13 nm), GNPs (60 nm), PEG-GNR were cultured with the adhered cells. Then, the cells were washed three times with PBS, collected using trypsin, and at the end centrifuged. The cell pellets were dissolved in aqua regia (AR) for the Au mass content by ICP-OES to assess the process of NPs cell uptake.

X-ray obserbtion property of the GNPs versus Omnipaque

Solutions of GNPs (13 nm) and conventional CT contrast media (Omnipaque 300 mg/ ml, GE Healthcare) with different concentrations (2500, 3000, 3500, 4000, 4500, 5000 μM) were ready in 0.5 ml Eppendorf tubes and located in a designed phantom. CT imaging was done using a 64-slice hospital CT modality (GE Healthcare).

Statistical analysis

For comparing the various groups to each other, a One-way ANOVA test was applied. A P value higher than 0.05 was considered not statistically significant. The GraphPad Prism 6 software (USA) carried out data measurements are mean ± standard deviation (SD). The analysis was carried out by the GraphPad Prism 6 software (USA).

RESULTS AND DISCUSSION
Synthesis and characterization of GNPs and GNRs

synthesized and characterized GNPs at two various sizes (13and 60 nm) with spherical morphology, GNRs at two various AR and PEGylated surfaces on GNRs was performed in the previous research[10]. Briefly, Raman spectroscopy and UV-visible corroborated the bond of PEG to the GNRs. The Formation and morphology of GNPs and GNRs were verified using exist of specific surface plasmon resonance (SPR) in UV-visible and TEM, respectively. The mean aspect ratio (AR) of
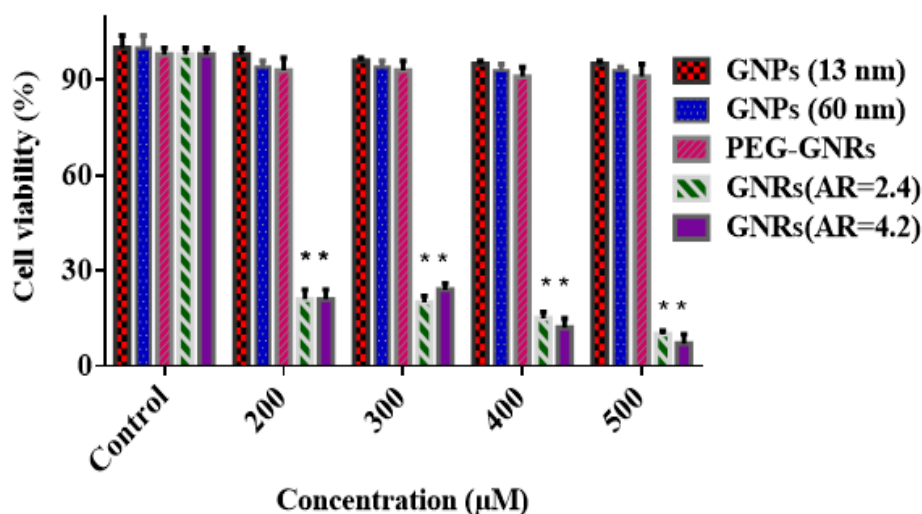
Fig. 1. MTT viability of KB cells after incubated with NPs with various concentrations range (0–500 µM. (n=3 replicated).

GNRs was ~2.0, which is in excellent agreement with an estimation of ~2.4 based on UV-Visible (surface plasmon resonance peak at ~647). Peaks attributed and C-O and Au-S bonds corroborated the binding of mPEG-SH ligand to the external area of GNRs[10].

Cytocompatibility assays

In biomedicine, cell viability is a principle and essential subject for a material. We measured the cytocompatibility of NPs on HDF and KB cells using cell viability assay, Survival fraction, and microscopic observation of change morphology. The cytotoxicity of GNPs (13 nm), GNPs (60 nm), PEG-GNR, GNR (2.4), and GNR (4.2) on the KB cell line was determined using MTT assay. Fig. 1 shows the toxicity of NPs at incubation time of 24 h. As shown, the synthesized nanoparticles (GNPs (13 nm), GNPs (60 nm), PEG-GNR were nontoxic at given concentrations range of 0-500 µM, no significant difference compared to the control group, but, GNRs (2.4) and GNRs (4.2) were toxic at the concentration range.

GNRs are commonly realized extremely cytotoxic because of using a very high concentration of Cetyltrimethylammonium Bromide (CTAB) in their synthesis[11]. We tried to remove the CTAB molecules using centrifugation, but its outcomes to lead modifies in shape, and size of particles[10]. Although, GNRs were washed several times, nevertheless they created toxicity. Accordingly, for reduce the cytotoxicity, the unbound CTAB molecules on the surface layer of

the NPs were covered by PEG molecules[10, 12].

The long-term cytotoxicity of GNPs (13 nm) was evaluated by a clonogenic assay. Fig. 2a shows an image of a colony of nasopharyngeal cells after 10 days using a microscope. NPs were non-toxic at a concentration of 500 µM, with no significant difference from the control group (Fig. 2 b).

As shown in Fig. 3, the microscopic image of H&E-stained HDF cells incubated with GNPs (13 nm) in the Au at different concentrations does not display considerable morphological changes in cells when compared and evaluated with the control.

X-ray absorbtion measurements of GNPs versus Omnipaque

The X-ray absorbtion intensity (XAI) properties of the GNPs (13 nm) was contrasted to a conventional small-molecule CT contrast media based on iodine (such as Omnipaque at different concentration of iodine or Au (2500, 3000, 3500, 4000, 4500 and 5000 µM). CT images of suspensions indicated that with the elevation of Au or iodine concentration, the contrast, and brightness of the CT images and the CT value (quantitative pixels) or the XAI of both Omnipaque and GNPs increased. Finally, the elevating trend of GNPs is higher in XAI (HU) than that of Omnipaque with a similar concentration range of the contrast media (Au or iodine). In this study, the XAI of the GNPs is nearly 3-times more remarkable than that of Omnipaque in the concentration of 5000 µM at the potential tube of 80 kVp (Fig. 4). Theoretically,
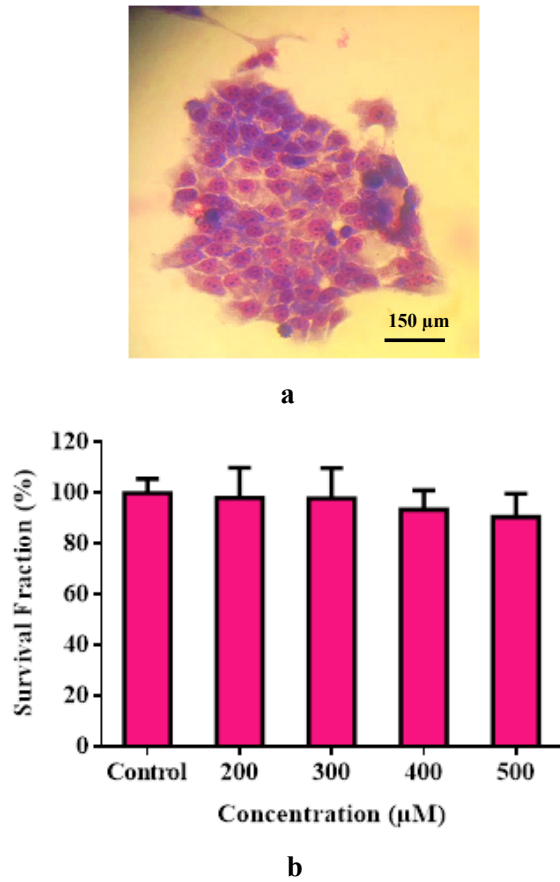
671

a

b

Fig. 2. (a) KB colony photograph microscopy after treatment 10 days after incubation of cells with GNPs (13nm) (400×). (b) Diagram of survival fraction of KB cells after incubation of GNPs (13 nm) at different concentration.

a) Control   **b) 200 μ M**   **c) 300 μ M**
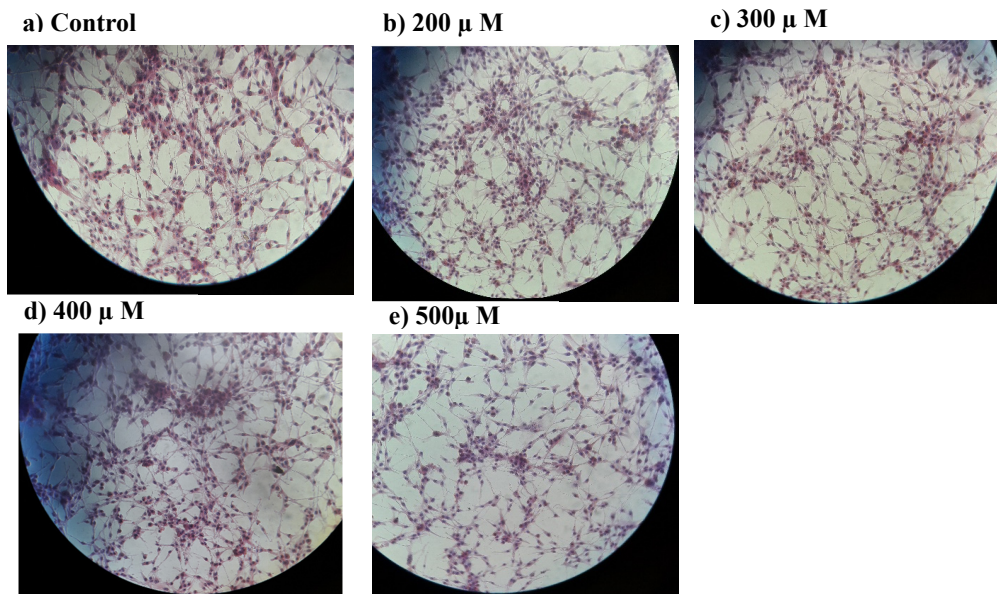

d) 400 μ M   **e) 500μ M**

Fig. 3. Representative microscopic images of H&E-stained HDF cells. Control cells without treatment and the cells incubated with GNPs (13nm) at the different concentrations range (2000×).
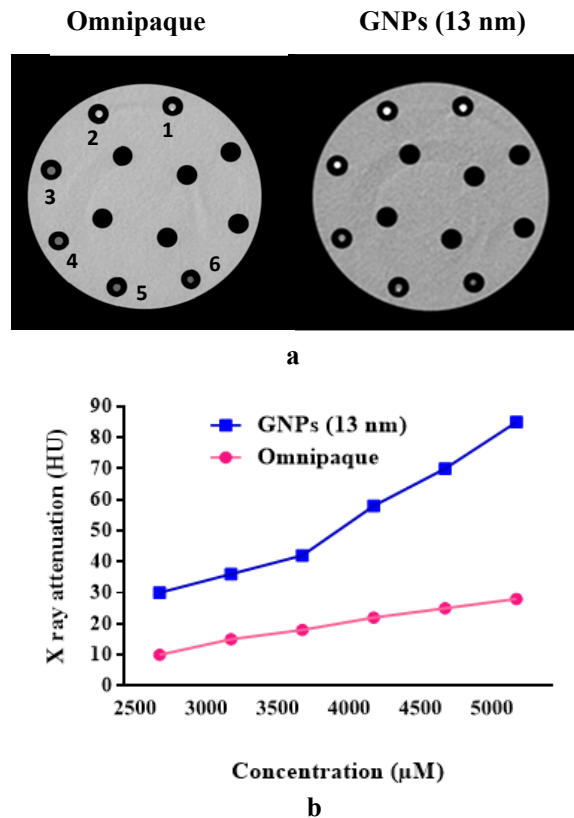
Omnipaque   **GNPs (13 nm)**

a

b

Fig. 4. (a) CT images of Omnipaque and GNPs at different concentration (µM) (1; 5000, 2; 4500, 3; 4000, 4; 3500, 5; 3000, and 6; 2500) at tube potential 80 kVp.(b) Diagram of the X-ray attenuation of Omnipaque versus GNPs.

Au has a higher XAI coefficient than iodine small molecule because of its higher atomic number and electron density (79 and 19.32 g/cm^3, respectively) than those of iodine (53 and 4.9 g/cm^3). It was revealed that with increasing concentration of the Omnipaque or conventional contrast media and GNPs, XAI increased[13]. Peng et al. evaluated the effect of iodine concentration on XAI. Their results indicated that XAI of Omnipaque is 150-times more signicant than that of PBS (control group such as water) at a concentration of 18,180 µg/ml at 100 kVp. There was a good correlation between CT number and concentration of the Omnipaque as a conventional based on iodine contrast media[12].

These findings suggest that the higher XAI property of the GNPs than that of Omnipaque is necessary for the quality and excellent sensitivity of CT scanning applications.

CT imaging of nasopharyngeal cancer cells

We next evaluated the possibility, and effect of using the formed PEG-GNR, GNPs (13nm), and GNPs (60 nm) for CT imaging of head and neck cancer cell lines. The KB cells were cultured with three NPs with various concentrations (0, 200, 300, 400, and 500 µM), 24 h incubation time and exposed at 80 kVp tube potential by a hospital CT imaging modality. Fig. 5a represents the coronal section of CT scanning images of KB cells incubated with NPs at various concentrations. As can be seen, it is clear from the coronal view that for three NPs, by increasing the concentration of NPs, XAI increased and is brighter. There is a statistically significant difference in XAI between any of the GNPs for any of the concentrations used. Our results demonstrated that smaller spherical GNPs (13 nm) had greater XAI than larger spherical GNPs (60 nm) and PEGylated GNRs. As shown in Fig. 5b, the XAI of the GNPs (13 nm) is approximately 2.55-times and 1.63-times greater than that of PEG-GNRs and GNPs (60 nm) in nasopharyngeal cancer cells, respectively, in the concentration of 500 µM at 80 kVp. Our results demonstrated that smaller spherical GNPs had higher CT values (XAI) than PEGylated GNRs and larger spherical shapes
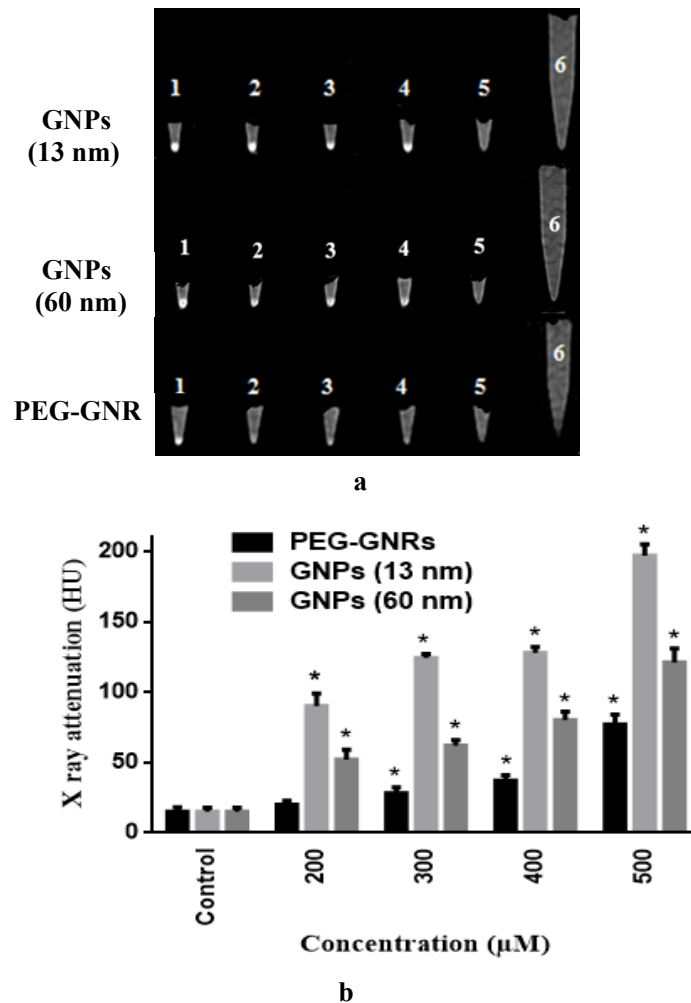
Fig. 5. (a)Coronal section images (a) and the HU (b) of KB cells cultured with NPs with various concentrations (μM) (a: 1; 200, 2; 300, 3; 400, 4;500, 5; control, 6; water) for 24h at tube potential tube of 80 kVp (n=3).

of GNPs. Overall, The smaller the GNPs, the higher X-ray attenuation.

There are few researches are performing on the effect of morphology and size of GNPs on X-ray attenuation. The size of GNPs can affect their biocompatibility, optical imaging properties, and efficiency for therapeutic applications[14]. Conflicting studies have been reported with regard to the effect of GNPs sizes on XAI. One study reported that there is no difference in XAI in radiography modality among GNPs at different sizes or morphology (sizes of 4, 6, and 25 nm, and nanorods of 63 nm in length and 30 nm in diameter) due to the percentage of surface atoms based on the average dimensions of each NPs sample[15]. However, one research reported that the XAI enhancement by smaller GNPs (4 nm)

was higher than that of larger NPs (20, 40, and 60 nm) at a similar concentration range [15]. Xu et al. reported that with the similar amount of element Au, CT value relies on the target site[16]. Accordingly, the smaller GNPs with greater external area exhibit more demonstrative CT value and X-ray attenuation. In other words, diminished GNPs diameter results in greater number of NPs in a similar bulk rather than larger GNPs of the similar concentration.

In the previous study, our findings indicated GNPs with smaller sizes have greater XAI than a larger one, and even than GNRs shape[10]. In this study, the effect of concentration, size, surface chemistry and morphology of NPs evaluated on nasopharyngeal cancer cells. Our findings demonstrated that HU (CT value) of GNPs (13
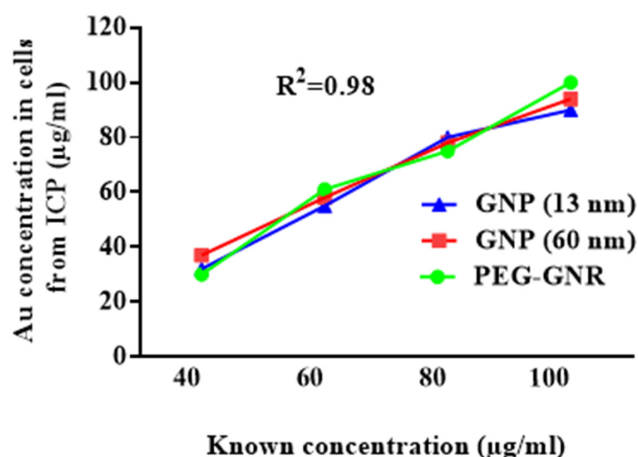
Fig. 6. ICP analysis of GNPs after incubation in KB cells.

nm) is approximately 2.55-times and 1.63-times higher than that of PEG-GNRs and GNPs (60 nm) in nasopharyngeal cancer cells, respectively, in the concentration of 500 µM at 80 kVp. XAI is a function of GNPs concentration showed a good-correlated linearity relation. Our findings revealed a higher mass concentration in the whole of the NPs results in greater XAI and led to NPs accumulation in the body at the target place. The precision of concentrations in KB cells was clarified by the ICP analysis. As shown in Fig. 6, measurement of gold concentrations from ICP agree with the gold concentrations incubated in cells. The XAI of GNPs is both concentration and size-dependent, with smaller GNPs at higher concentrations presenting excellent effect.

Xia et al. in 2011 and Huang et al. in 2014 evaluated the different concentrations of GNRs (0–3000 µg/ml) and (0–200 µg/ml), respectively, for CT imaging. Their results demonstrated that by elevating the element concentration, XAI enhanced and led to brighter CT images [17, 18]. Since the CT imaging has a potency of 4096 gray levels, that prepared various density rates in CT value (HU) and the human eye can only recognize 20 gray levels in CT image[13]. This is hard to visually distinguish the brightness of the KB cells cultured with GNPs with various concentrations. Fortunately, the HU value, as a quantitative average that shows the actual XAI of the target, is rather specific, accurate, and reliable than the image. Quantitative analysis (QA) of the HU should be performed with the standard and specified display program. In the previous study, GNRs with a higher aspect ratio has a greater XAI. As described

before, the cytotoxicity of GNRs depends on their surface chemistry. Accordingly, in the previous study, PEGylated GNRs were synthesized, and their XAI (without cells) was investigated while CTAB was removed. When the PEGylation was performed on GNRs with larger AR, the PEGylated GNRs demonstrated much lower CT value than small and large AR of GNRs. This can be ascribed to the existence of CTAB molecules on the external of GNRs in the form of double layer, which can simplify edge to edge arrangement of the GNRs, which reads to behave like longer structures with greater CT value or XAI[10]. This did not occur when GNRs were covered with PEG, and accordingly, a smaller XAI was calculated. GNRs with larger AR were also shown to have higher CT values, which can be related to their higher Au content in contrast to smaller NPs.

GNPs are a promising platform in nanomedicine capable of integrating multiple diagnostic functions. The facile and tuneable preparation, bioinert, easy surface modification, nontoxic, and strong X-ray attenuation properties make GNPs a potentially ideal contrast media[19]. Moreover, GNPs could benefit from the immature structure of tumor vasculature, and selectively locate at the tumor site by the enhanced permeability and retention (EPR) effect. Structural characteristics (surface functionalization, shape and size) plus the concentration of NPs can influence CT value. The XAI of high atomic number materials is ascribed to their higher electron density relied on X-ray photoelectric effect (PE)[1, 14].

Different gold structures (nanoshells, nanocages and nanorods) have primary use in

biomedicine applications, such as theranostic (delivery of drug and diagnostic)[20]. For instance, GNRs were applied for synchronous X-ray imaging, and photothermal therapy to show a high absorbtion cross-section in the near-infrared region (NIR) [21]. The synthesis of GNPs with multifunctional usage is an essential part of a study with considerable emphasis on multimodal and theranostic agents. Therefore, it is necessary to apply suitable sizes and morphologies to increase X. Our findings can be used for the usage of gold nanostructures in radiotherapy (radiation dose enhancement (RDE)), where NPs with high XAI is performed.

Because of hospital CT modality has a nearly low resolution (0.625 mm) in contrast to preclinical CT or micro-CT (45 μM) and since the preclinical CT has not been really applied in the hospital, these findings have a high potential for utilizing in the clinic.

CONCLUSION

In summary, we evaluated the effect of morphology, concentration, surface chemistry, and size of GNPs on X-ray attenuation in human nasopharyngeal cancer cells. Morphological observation of cells after H&E staining, MTT, and colony assays of cell viability demonstrated that different concentrations of GNPs (13 nm), GNPs (60 nm) and PEG-GNR do not affect cell viability, and morphology. Their parameters reflected their excellent compatibility at the given concentration level. However, GNRs (2.4) and GNRs (4.2) due to CTAB were toxic. Higher XAI property of GNPs (13 nm) than that of the Omnipaque under the similar concentration provides beneficial CT imaging. XAI increased when mass concentration of NPs elevated. Based on our study, the XAI of GNPs (13) is greater than GNPs (60nm) and PEG-GNR in KB cancer cells. The XAI of GNPs depends on both higher concentrations with the smaller sizes until presenting excellent effects in the image. In sum, smaller spherical GNPs can be proposed as an excellent possibility to Omnipaque for CT imaging of nasopharyngeal cancer cells. In order to gain clinical acceptance, further *in vivo* studies must be performed.

ACKNOWLEDGMENTS

CONFLICT OF INTEREST

The authors declare that there is no conflict of interests regarding the publication of this manuscript.

REFERENCES

1. Beik J, Jafariyan M, Montazerabadi A, Ghadimi-Daresajini A, Tarighi P, Mahmoudabadi A, et al. The benefits of folic acid-modified gold nanoparticles in CT-based molecular imaging: radiation dose reduction and image contrast enhancement. Artificial cells, nanomedicine, and biotechnology. 2018;46(8):1993-2001.

2. Khademi S, Sarkar S, Shakeri-Zadeh A, Attaran N, Kharrazi S, Ay MR, et al. Targeted gold nanoparticles enable molecular CT imaging of head and neck cancer: an in vivo study. The international journal of biochemistry & cell biology. 2019;114:105554.

3. Bouché M, Hsu JC, Dong YC, Kim J, Taing K, Cormode DP. Recent advances in molecular imaging with gold nanoparticles. Bioconjugate Chemistry. 2019;31(2):303-314.

4. Yu Y, Yang T, Sun T. New insights into the synthesis, toxicity and applications of gold nanoparticles in CT imaging and treatment of cancer. Nanomedicine. 2020;15(11):1127-1145.

5. Lee N, Choi SH, Hyeon T. Nano-sized CT contrast agents. Adv Mater. 2013;25(19):2641-2660.

6. Khademi S, Sarkar S, Shakeri-Zadeh A, Attaran N, Kharrazi S, Solgi R, et al. Dual-energy CT imaging of nasopharyngeal cancer cells using multifunctional gold nanoparticles. IET nanobiotechnology. 2019;13(9):957-961.

7. Moghimi SM, Hamad I. Factors controlling pharmacokinetics of intravenously injected nanoparticulate systems. Nanotechnology in drug delivery: Springer; 2009. p. 267-282.

8. Albanese A, Tang PS, Chan WC. The effect of nanoparticle size, shape, and surface chemistry on biological systems. Annu Rev Biomed Eng. 2012;14:1-16.

9. Sonavane G, Tomoda K, Makino K. Biodistribution of colloidal gold nanoparticles after intravenous administration: effect of particle size. Colloids Surf B Biointerfaces. 2008;66(2):274-280.

10. Khademi S, Sarkar S, Kharrazi S, Amini SM, Shakeri-Zadeh A, Ay MR, et al. Evaluation of size, morphology, concentration, and surface effect of gold nanoparticles on X-ray attenuation in computed tomography. Phys Med. 2018;45:127-133.

11. Yasun E, Li C, Barut I, Janvier D, Qiu L, Cui C, et al. BSA modification to reduce CTAB induced nonspecificity and cytotoxicity of aptamer-conjugated gold nanorods. Nanoscale. 2015;7(22):10240-10248.

12. Peng C, Qin J, Zhou B, Chen Q, Shen M, Zhu M, et al. Targeted tumor CT imaging using folic acid-modified PEGylated dendrimer-entrapped gold nanoparticles. Polymer Chemistry. 2013;4(16):4412-4424.

13. Khademi S, Sarkar S, Shakeri-Zadeh A, Attaran N, Kharrazi S, Ay MR, et al. Folic acid-cysteamine modified gold nanoparticle as a nanoprobe for targeted computed tomography imaging of cancer cells. Materials Science and Engineering: C. 2018;89:182-193.

14. Dong YC, Hajfathalian M, Maidment PS, Hsu JC, Naha PC, Si-

Mohamed S, et al. Effect of gold nanoparticle size on their properties as contrast agents for computed tomography. Sci Rep. 2019;9(1):1-13.

15. Jackson P, Periasamy S, Bansal V, Geso M. Evaluation of the effects of gold nanoparticle shape and size on contrast enhancement in radiological imaging. Australas Phys Eng Sci Med. 2011;34(2):243.

16. Xu C, Tung GA, Sun S. Size and concentration effect of gold nanoparticles on X-ray attenuation as measured on computed tomography. Chem Mater. 2008;20(13):4167-4169.

17. Huang P, Bao L, Zhang C, Lin J, Luo T, Yang D, et al. Folic acid-conjugated silica-modified gold nanorods for X-ray/CT imaging-guided dual-mode radiation and photo-thermal therapy. Biomaterials. 2011;32(36):9796-9809.

18. Xia H-X, Yang X-Q, Song J-T, Chen J, Zhang M-Z, Yan D-M, et al. Folic acid-conjugated silica-coated gold nanorods and quantum dots for dual-modality CT and fluorescence imaging and photothermal therapy. Journal of materials chemistry b. 2014;2(14):1945-1953.

19. Beik J, Khademi S, Attaran N, Sarkar S, Shakeri-Zadeh A, Ghaznavi H, et al. A nanotechnology-based strategy to increase the efficiency of cancer diagnosis and therapy: folate-conjugated gold nanoparticles. Curr Med Chem. 2017;24(39):4399-4416.

20. Dou Y, Guo Y, Li X, Li X, Wang S, Wang L, et al. Size-tuning ionization to optimize gold nanoparticles for simultaneous enhanced CT imaging and radiotherapy. ACS nano. 2016;10(2):2536-2548.

21. Shang T, Wang C-d, Ren L, Tian X-h, Li D-h, Ke X-b, et al. Synthesis and characterization of NIR-responsive Au rod@ pNIPAAm-PEGMA nanogels as vehicles for delivery of photodynamic therapy agents. Nanoscale research letters. 2013;8(1):1-8.